



Segregation of alloying elements to intrinsic and extrinsic stacking faults in γ' -Ni₃Al via first principles calculations

N.C. Eurich and P.D. Bristowe*

Department of Materials Science and Metallurgy, University of Cambridge, Cambridge CB3 0FS, United Kingdom

Received 26 November 2014; revised 27 January 2015; accepted 14 February 2015

Available online 3 March 2015

First principles calculations are used to investigate the segregation behaviour of Co, Cr, Re, Mo and W to intrinsic and extrinsic stacking faults in γ' -Ni₃Al. It is shown that the change in stacking fault energy depends on local alloying concentration and is related to subtle changes in the electronic structure of the alloying elements and adjacent nickel atoms. The results are consistent with observed stacking fault segregation in commercial superalloys and in particular the behaviour of Co and Cr.

© 2015 Acta Materialia Inc. Published by Elsevier Ltd. This is an open access article under the CC BY license (<http://creativecommons.org/licenses/by/4.0/>).

Keywords: CMSX-4; Ni₃Al; Stacking faults; Segregation; First principles calculations

It has been shown recently [1] using energy dispersive X-ray spectroscopy (EDS) that the distribution of alloying elements in the vicinity of intrinsic stacking faults (SISFs) within the γ' phase (Ni₃Al) of two commercial superalloys (CMSX-4 and ME3) following creep deformation at around 700 °C can vary significantly. While the segregation of heavy (high-Z) elements to extrinsic faults (SESF) in γ' in CMSX-4 has been reported previously [2], the recent analysis by Viswanathan et al. [1] provided clear experimental evidence for an enhanced concentration of particular elements, notably Co and Cr, near SISFs with a simultaneous reduction in the amount of Ni and Al. Although it was suggested that the formation of these faults and long-range diffusion of the segregants were closely connected, no clear physical picture emerged of why it is energetically favourable for these elements to segregate and others not. On the theoretical side there is a substantial literature [3–5] using atomistic modelling which describes the effect of alloying elements on stacking faults and anti-phase boundaries in γ' -Ni₃Al but the specific interaction of Co and Cr has not yet been investigated.

To gain better understanding at the electronic level of the observed effects, first principles atomistic calculations are employed to determine the relative driving force for segregation of Co and Cr to SISFs and SESFs in γ' -Ni₃Al. For comparison calculations are also performed on the segregation of Mo, W and Re. These elements are all standard components of CMSX-4 (and also ME3 except Re) and thus the results are also highly relevant to the experimentally observed segregation of high-Z elements to SESFs [2,6].

Gaining an understanding of the effect of alloying elements not only on intrinsic but also on extrinsic stacking faults is of particular interest because of the experimental finding that the shearing of γ' precipitates via the creation of SESFs is an important deformation mechanism at intermediate temperature service conditions in both polycrystalline Ni-based alloys for disc applications [7] as well as single crystal alloys [8] used as materials for turbine blades.

γ' -Ni₃Al is based on the L1₂ crystal structure with Al atoms occupying the corners and Ni atoms the faces of a fcc unit cell. Both extrinsic and intrinsic stacking faults occur on the (111) glide plane and consist of a stacking irregularity in the threefold ABC stacking sequence. The SISF corresponds to the removal, and the SESF to the insertion of a close-packed plane of atoms. The computational cell is therefore constructed to consist of 11 and 13 close-packed layers of Ni₃Al with stacking sequences ABC ABC A|C ABC and ABC ABC AB|A|C ABC for the SISF and SESF respectively as shown in Figure 1 and is periodic in all directions. Test calculations were performed to ensure that the supercells are large enough along [111] to minimise the interaction of the fault with its periodic image.

To simulate the effect of alloying concentration on the segregation behaviour two different model sizes in the (111) plane were used. The standard model (SM) has one repeat unit in the (111) plane (i.e. 4 atoms/layer) while the larger model has four repeat units (16 atoms/layer). A single alloying atom is substituted into both models. A higher alloying concentration is modelled by introducing two alloying atoms into the standard model and this is referred to as the high concentration model (HM). Defining the stacking fault region as 4 (111) planes

* Corresponding author; e-mail: pdb1000@cam.ac.uk

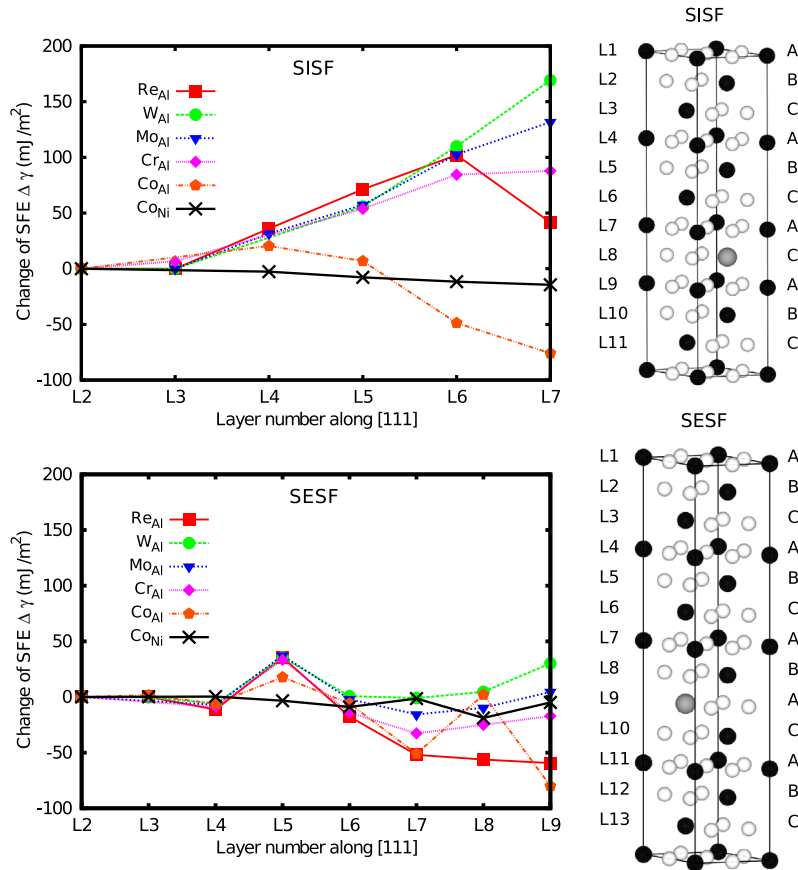


Figure 1. Change in SFE for the SISF (top) and the SESF (bottom) as a function of (111) layer number for the five alloying elements considered. Also shown are atomic models of the SISF and SESF used in the calculations. *ABC* refers to the stacking sequence of (111) planes and L1–L13 indicates the layer number. For the SISF the fault lies between L7 and L8 and for the SESF the fault lies at L9. Open, black and coloured circles refer to Ni, Al and alloying elements respectively. (For interpretation of the references to colour in this figure legend, the reader is referred to the web version of this article.)

(*CA|CA* for the SISF and *AB|A|C* for the SESF) then the local alloy concentration is about 1.6 at.%, 6.25 at.% and 12.5 at.% for the LM, SM and HM respectively. The question of whether the alloying elements considered in this work preferentially substitute for Al or Ni sites in bulk Ni_3Al has been widely considered both experimentally [9] and theoretically [10]. Most theoretical studies agree that Cr, Re, Mo and W preferably substitute on the Al sublattice while the site preference of Co is commonly found to be composition dependent and thus Co may substitute on either the Al or Ni sublattice. Therefore elements are substituted for Al sites only if the site preference is unambiguous (Cr, Re, W and Mo), and for both Ni and Al sites where the site preference is composition dependent (Co).

All calculations in this work were performed using the CASTEP code [11] which implements the plane wave pseudopotential methodology of the density functional theory (DFT). The PBE generalised gradient exchange correlation functional [12] was used along with Vanderbilt-type ultra-soft pseudopotentials [13]. The plane wave kinetic energy cut-off was converged to 500 eV and the Brillouin zone was sampled using a k -point spacing of 0.04 \AA^{-1} in reciprocal space. For the atomic relaxations the tolerances for energy change, maximum displacement and maximum force were set to 1.0×10^{-5} eV/atom, 1.0×10^{-3} Å and 0.03 eV/Å,

respectively. In order to account for the ferromagnetism of Ni all segregation energy calculations were performed using spin polarisation, starting at a ferromagnetic initial configuration and relaxing towards its ground state. The SISF and SESF energies of pure Ni_3Al are calculated to be 68 mJ m^{-2} and 89 mJ m^{-2} , respectively, in good agreement with other computational results [14].

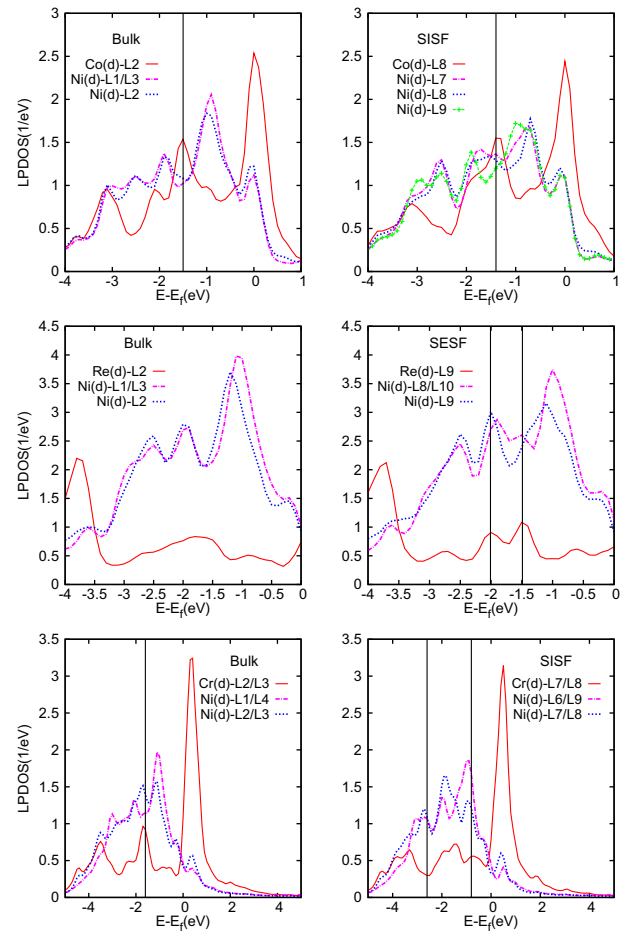
In order to quantify the propensity for segregation, the change in stacking fault energy (SFE) $\Delta\gamma$ due to the incorporation of 1 (or 2) alloying atoms into the models is calculated using the approach used previously for antiphase boundaries and complex stacking faults [3]. A negative change in SFE implies segregation. Example locations for a single alloying atom placed into the SISF and SESF fault plane are shown in Figure 1 using the SM. Also shown in Figure 1 is $\Delta\gamma$ as a function of distance from both faults following the introduction of a single alloying atom for all five elements considered. For the SISF it is seen that the effect is largest for all elements (except Re) when the atom is placed directly into the fault plane (L7). The only element to reduce the SFE is Co_{Al} . The overall width of the segregation profile for Co_{Al} is about 6 layers (~ 1.5 nm) which is consistent with measured profiles in CMSX-4 and ME3 [1]. For the SESF the calculated values of $\Delta\gamma$ are much smaller but again Co_{Al} reduces the SFE when placed in the fault plane (L9) as does Re.

Table 1. Values of the change in stacking fault energy $\Delta\gamma$ due to the incorporation of one (or two) alloying atoms in the fault plane. LM, SM and HM refer to models with increasing alloy concentrations as described in the text.

Alloying element	$\Delta\gamma_{\text{SISF}}^{\text{LM}}$	$\Delta\gamma_{\text{SESF}}^{\text{LM}}$	$\Delta\gamma_{\text{SISF}}^{\text{SM}}$	$\Delta\gamma_{\text{SESF}}^{\text{SM}}$	$\Delta\gamma_{\text{SISF}}^{\text{HM}}$	$\Delta\gamma_{\text{SESF}}^{\text{HM}}$
Co _{Al}	12	−18	−77	−80	−95	−102
Co _{Ni}	−4	−5	−8	−5	−46	−65
Cr _{Al}	48	20	85	−17	−126	−135
W _{Al}	77	22	171	30	−68	−106
Re _{Al}	60	19	46	−60	−277	−229
Mo _{Al}	73	17	138	5	−126	−139

Table 1 summarises the values $\Delta\gamma$ specifically for substitution of the alloying atom into the fault plane and also includes data for the large and high concentration models. For the large model where the alloy concentration is reduced it is clear that only Co weakly segregates to the stacking faults. The non-segregation of the heavy elements W, Re and Mo agrees with previous calculations on the SISF [4,5]. Table 1 also gives the results for the HM model where the two alloying atoms are specifically placed in L7 and L8 for the SISF and L8 and L9 for the SESF. In these cases all the elements considered apparently decrease the SFE and thus segregate to both stacking faults. However, these results must be viewed with caution since the solubility limits [9] of some of the elements (notably W, Re and Mo) may have been exceeded and as discussed previously this can lead to unreliable segregation energies [15]. Nevertheless for Co and Cr, which have higher solubilities, it is clear that segregation will occur to both faults once the concentration is high enough which agrees with the recent observations on SISFs [1]. In addition to the layer combinations mentioned above, two alloying atoms were also placed in L5–L7, L6–L7 and L6–L8 for the SISF and L8–L10 and L9–L11 for the SESF. This allowed access to a greater range of possible double segregation sites. The results reveal that for the SISF, placing Co and Cr in L7–L8 is still preferred energetically although the other layer combinations still lead to segregation. Overall, the segregation of Co and Cr to the SISF may occur at many local sites extending over about 6 layers which is consistent with the microscopy (HAADF) images [1]. For the SESF it is found that all the alloying elements including Co_{Al} and Cr prefer the L9–L11 combination rather than L8–L9 which is of interest because this arrangement corresponds to a particular hexagonal structure with X–Al–X–Al ordering of Al and heavy elements X over the prototype Ti sites of the underlying D0₂₄ structure called the η phase [16] whose observation was suggested previously in the context of heavy element segregation to SESFs [2].

To gain a better understanding of the calculated segregation effects at the electronic level, the layer-by-layer projected density of states (LPDOS) across each stacking fault is determined using OPTADOS [17] focussing on the observed segregation of Co and Cr to the SISF and Re to the SESF. Of interest is the absence or presence of hybridisation effects which may indicate a weakening or strengthening of bonds adjacent to the alloying element. However, the effects are expected to be relatively subtle since, unlike segregation to anti-phase boundaries or complex stacking faults [3], no new alloy-host bonds are broken or created. For reference, the left hand side column of Figure 2 shows the effects of substituting Co, Cr and Re into bulk Ni₃Al on Al sites away from the fault. The alloying atom is in layer 2 (L2) of the model (and also L3 for Cr) and the DOS shows

**Figure 2.** The layer-by-layer projected density of states (LPDOS) for the d-orbitals of the Co, Re and Cr alloying elements compared to adjacent Ni atoms in the bulk region of the model (left column) and at the stacking faults (right column). The layer numbers are defined in Figure 1. The full vertical lines indicate possible resonances between orbitals. E_f is the Fermi energy.

the projected d-orbitals of this atom and the nearest neighbour Ni atoms. Since all optimisations converged to a non-magnetic ground state the spin-up and spin-down DOS are equal and thus only the spin-up component is shown. The right hand side column of Figure 2 shows the effects of substituting Co into a SISF (L8), Re into a SESF (L9) and two Cr atoms into a SISF (L7 and L8) all on Al sites.

When Co is introduced into the SISF it is found to segregate (using the standard model) and evidence for this in the DOS is found by examining the energies of the Ni(d) states around the main Co(d) peak at -1.5 eV (top two

panels of Fig. 2). In the bulk region the Co(d) resonance coincides with an energy minimum in the Ni(d) states of the neighbouring Ni atoms whereas at the SISF the energies of two of these Ni(d) states increase, broaden out and hybridise with the Co(d) state. This suggests enhanced bonding between the Co atom and its Ni neighbours thus favouring segregation.

A similar situation occurs when Re is substituted into the SESF (using the standard model). In the bulk region the Re(d) states exhibit only a broad maximum between -2 eV and -1.5 eV which coincide with an energy minimum in the Ni(d) states of the neighbouring Ni atoms whereas at the SESF the Re(d) states develop two resonances at -1.3 eV and -1.9 eV, the latter strongly matching a resonance of Ni(d) states (middle two panels of Fig. 2). The Re(d) peak at -1.3 eV correlates with small enhancement Ni(d) states which together with the strong resonance enhances the local bonding and rationalises the tendency of Re to segregate towards the SESF.

When two Cr atoms are introduced into the SISF using the high concentration model strong segregation is observed. The bottom two panels of Figure 2 show that in the bulk region the Cr(d) states exhibit a narrow peak at -1.8 eV which coincides with a resonance of Ni(d) states belonging to the Ni atoms lying in the same close-packed plane as the incorporated Cr. It is noticeable, however, that the overlapping Ni(d) states between Ni atoms that lie within (L2 and L3) and adjacent (L1 and L4) to the planes containing Cr is weak, e.g. the peak of Ni(d) (L2 and L3) at -1.8 eV coincides with a minimum of Ni(d) states of Ni atoms lying in planes L1 and L4. This situation changes at the SISF where it is seen that the resonance peaks of Ni(d) states of Ni atoms in the fault (L7 and L8) and in planes adjacent to it (L6 and L9) coincide. Furthermore it is seen that the narrow Cr(d) peak broadens and matches with a widened peak associated with Ni(d) states from the Ni atoms in the fault (L7 and L8). The combined effects provide evidence for stronger local bonding that favours segregation.

The analysis shows that even small changes in stacking fault energy can be related to features in the electronic structure of the alloying elements and stacking faults and are consistent with the observed segregation behaviour.

Support for this work was provided by the EPSRC/Rolls-Royce Strategic Partnership. The calculations were performed using the high performance computing facilities at the University of Cambridge and the UK national facility ARCHER. Access to the latter was obtained via the UKCP consortium and funded by EPSRC grant EP/K014560/1. The authors wish to thank Dr. Cathie Rae for useful discussions.

- [1] G.B. Viswanathan, R. Shi, A. Genc, V.A. Vorontsov, L. Kovarik, C.M.F. Rae, M.J. Mills, *Scr. Mater.* 94 (2015) 5.
- [2] V.A. Vorontsov, L. Kovarik, M.J. Mills, C.M.F. Rae, *Acta Mater.* 60 (12) (2012) 4866.
- [3] X.-X. Yu, C.-Y. Wang, *Philos. Mag.* 92 (2012) 4028.
- [4] X.-X. Yu, C.-Y. Wang, *Mater. Sci. Eng. A* 539 (2012) 38.
- [5] Y.-F. Wen, J. Sun, J. Huang, *Trans. Nonferrous Met. Soc. China (English Edition)* 22 (2012) 661.
- [6] L. Kovarik, R. Unocic, J. Li, P. Sarosi, C. Shen, Y. Wang, M. Mills, *Prog. Mater. Sci.* 54 (2009) 839.
- [7] B. Décamps, S. Raujol, A. Coujou, F. Pettinari-Sturmel, N. Clément, D. Locq, P. Caron, *Philos. Mag.* 84 (2004) 91.
- [8] C.M.F. Rae, R.C. Reed, *Acta Mater.* 55 (2007) 1067.
- [9] S. Ochiai, Y. Oya, T. Suzukoi, *Acta Metall.* 32 (1984) 289.
- [10] Q. Wu, S. Li, *Comput. Mater. Sci.* 53 (2012) 436.
- [11] S.J. Clark, M.D. Segall, C.J. Pickard, P.J. Hasnip, M.J. Probert, K. Refson, M.C. Payne, *Z. Kristallogr.* 220 (2005) 567.
- [12] J.P. Perdew, K. Burke, M. Ernzerhof, *Phys. Rev. Lett.* 77 (1996) 3865.
- [13] D. Vanderbilt, *Phys. Rev. B* 41 (1990) 7892.
- [14] R. Voskoboynikov, *Phys. Met. Metall.* 114 (2013) 545.
- [15] P. Lejcek, M. Sob, V. Paidar, V. Vitek, *Scr. Mater.* 68 (2013) 547.
- [16] N.C. Eurich, P.D. Bristowe, *Scr. Mater.* 77 (2014) 37.
- [17] A.J. Morris, R.J. Nicholls, C.J. Pickard, J.R. Yates, *Comput. Phys. Commun.* 185 (2014) 5.